Seismic vulnerability and fragility assessment of a strategic building in Algeria

Réception : 10/05/2023 Acceptation : 22/05/2023 Publication : 20/06/2023

BENBOKHARI Abdellatif[1], BENAZOUZ Chikh[1], MEBARKI Ahmed[2, 3] and REMKI Mostapha[4]

[1] Laboratoire des Travaux Publics, Ingénierie de Transport et Environnement - École Nationale Supérieure des Travaux Publics, Kouba, Algiers, Algeria.
[2]University Gustave Eiffel, UPEC, CNRS, Laboratory Modélisation et Simulation Multi Echelle (MSME 8208 UMR), Marne-la-Vallée, France.
[3]Nanjing Tech University (China), Permanent Guest Professor within "High-Level Foreign Talents Programme" grant.
[4] Centre National de Recherche Appliquée en Génie Parasismique (CGS), Algiers, Algeria.

Abstract

Purpose - The purpose of this paper is to assess the vulnerability and fragility of an existing strategic reinforced concrete (RC) civil protection building in Algeria, and to determine its suitability to the Algerian seismic regulations and its functionality during an earthquake event. The (IIZIS / CGS) methodology was implemented and used to analyze the building's capacity and nonlinear behavior by selecting three ground motions and defining four damage states. Earthquake records were expressed in terms of spectral values, and fragility curves were developed using the Risk-UE LM2 method. Additionally, a new step was added to the IIZIS / CGS methodology to estimate the repair cost of the building using a damage factor. The results of the assessment show the Department of Civil Protection building does not meet the requirements for resistance and deformability recommended by the CGS/IIZIS methodology for the group of users it serves. The addition of the damage factor allows for the calculation of repair costs, which can be used to determine whether the building should be strengthened or demolished.

The originality of this paper lies in the use of the IIZIS / CGS methodology to assess the vulnerability and fragility of an existing RC civil protection building, as well as the addition of a new step to the methodology that estimates repair costs using a damage factor. This information can be used to make informed decisions about the functionality of the building after an earthquake.

Keywords : Strategic building, Vulnerability, Capacity curve, fragility Curves, Nonlinear dynamic analysis, Damage factor

1. 1-Introduction

Over the past few decades, the losses caused by the natural catastrophes have increased dramatically around the world [1]. Earthquakes represent the most dangerous phenomenon among these catastrophes that are randomly happened unexpectedly with different intensities [2][3].

In Algeria, since the catastrophic earthquake [4][5] (Boumerdes 2003), where 2,300 people were killed, 11,000 injured, and 200,000 homeless. The seismic vulnerability assessment of existing buildings (specially the strategic buildings) became a serious step. The Algerian government started to invest in retrofitting and strengthening the strategic buildings, in order to prevent any economic damages or human losses [6]. Figure 1 represents the economic damages caused by earthquakes, aftershocks, and tsunamis as a share of GPD in the world in 2003 [7].

The seismic vulnerability of structures can be defined as its susceptibility to damages resulting from an earthquake event [8][9] [10]. It can be affected by many parameters, such as: (limited data collections, seismic hazard, soil type, the structural system, and plane and elevation regularity) [11].

Nowadays, depending on the scale study i.e.: individual building or territorial scale, there is

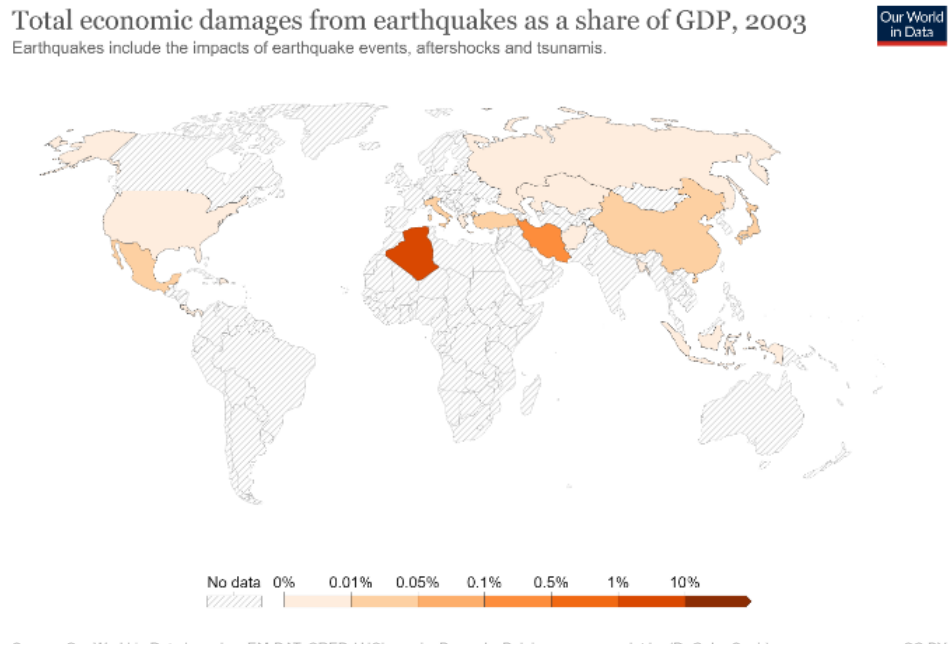

Figure 1 : Total economic damages (% GPD) in the world-2003[7].

An enormous amount of deterministic and probabilistic methodologies to assess the buildings' seismic vulnerability depending on the amount of the collected data, and the study area. Many procedures have been developed around the world, based on quantitative or qualitative estimation, [12], [13], [14], [15], [16], [17], [18], [19], [20] [21], [22], [23], [24])

In general, there are two main categories of the used methods: empirical and analytical categories. The empirical methods are usually considered as rapid methodologies that can give a realistic vulnerability assessment, but it may lead to inaccurate results in case of lack of data. Analytical methods are known as the most accurate methodologies that can consider all types of uncertainties, but they are time consuming and very sensitive to the input parameters. In addition, the empirical and analytical method can be combined in what we call hybrid methods (Biglari, Seismic vulnerability assessment and fragility analysis of Iranian historical mosques in Kermanshah city, 2022). Choosing a vulnerability assessment methodology involves considering the building typologies, the quality of the available information, and the computational effort that would be required.

In this paper, a civil protection building will be assessed using the (IIZIS/CGS) methodology, in order to check its functionality and its seismic capacity. The building is considered as a strategic building, and its functionality during and after an earthquake should be guaranteed with no extensive damages. Nonlinear static and dynamic analysis will be used to check its capacity compared to the demand and its dynamic response (displacement). Next, fragility curves will be constructed to estimate the probability of exceedance of each damage state using RISK-UE LM2.Finally, a damage factor will be proposed to be added in this method in order to have a repair cost estimation and to make the report more comprehensive for the administrative authorities.

2-Methodology for evaluating a building's seismic vulnerability

The IIZIS/CGS methodology is used to assess the seismic vulnerability of existing buildings. it was developed in partnership between the National Centre of Applied Research in Earthquake Engineering "C.G.S" (Algiers, Algeria), and IIZIS University (Republic of Macedonia) ([25]) ([26]). This methodology is based on the four main components of the seismic hazard assessment: seismic hazard definition, safety criterion, the earthquake scenario, structural building safety and damage analysis.

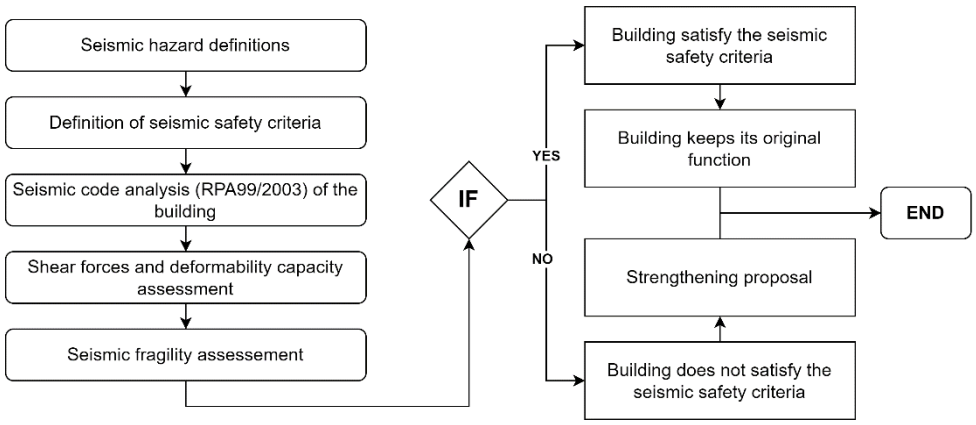

Figure 2 : The flowchart of the IIZIS/CGS methodology.

Fig. 2 illustrates the flowchart of the used methodology.

2.1. seismic hazard definition and safety criterion

A definition of attenuation laws and the seismic hazard were used to determine the maximum ground acceleration, for return periods of 100 and 500 years, [27] [28] [29] [30]). Fig. 3 shows the seismic hazard map according to the Algerian seismic code, and the location of the city (Constantine) is illustrated in fig. 4.

For the safety criterion, two (02) levels are generally determined for the seismic action:

The first level, the building is expected to be subjected to moderate earthquakes several times within its lifetime, with a return period of 100 years. As a result, the PGA is fixed at Amax=0.15g. Structures should behave elastically, allowing immediate use without any damage to the building.

The second level corresponds to major earthquakes that are expected to happen once during the building's life, with a return period of 500 years. The PGA is fixed as Amax=0. 25g. It is necessary to carry out dynamic and static analyses of the building and compare them to its capacity for moderate and major ground motions.

For the purpose of this study, a set of ground motion records was carefully chosen and employed :

- Imperial- Valley(USA) "North" 1940. [31]
- Trinidad (Trinidad and Tobago) "North" 1982. [31]
- Constantine (Algeria) N-S 1985. [31]

The characteristics of the selected ground motions are mentioned (name of earthquake, country, Station, duration (seconds) and maximum acceleration in Tab.1. Fig.5a and Fig.5b represent the selected earthquake ground motions spectra and the correspond accelerogram of the used earthquakes respectively.

Table 1 : Characteristics of selected motions.

Earthquake	Country	Station	Duration	Amax (m/sec²)
Imperial-Valley	USA	El-Centro	40	3.42
Constantine	Algeria	CEM-Abdelemoumn	20	2.86
Trinidad	Trinidad	090 CDMG	21	1.89

Tab.2 defines the maximum story drift displacement for the first and the second level.

Table 2 the maximum story drift displacement

First level	Second level
Story drift displacement	**Story drift displacement**
Δ_m= [H/400 & H/300]	Δ_M= [H/150 & H/125]

2.2- Structural analysis

The Algerian seismic code (RPA 1999/version 2003)(CGS, 2003) is used to check the structural elements of the building. If available M, Q, and N demands will be calculated based on horizontal seismic forces and compared to

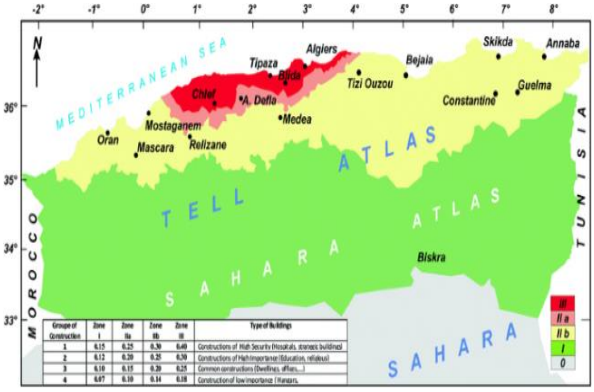

Figure 3 : The Algerian seismic hazard according to (RPA99/2003) in the term of peak ground acceleration (g) and the corresponding hazard zones. (19)

The initial design data. In the case of satisfied safety criteria, a final decision will be made based on the qualitative evaluation.

2.3- Vulnerability assessment

Dynamic response analysis represents a numerical computation to determine the linear and nonlinear behaviour of the structures. The definition of masses, stiffness and damping are required to calculate the structure's response (displacements, forces, and accelerations). A finite element method is recommended to determine the shear forces and the displacements of each story.

2.4. Seismic fragility analysis

The seismic fragility assessment is the final step of this methodology. Fragility curves will be constructed to evaluate the state of the building after an earthquake. The damage probability values, and damage factor will be calculated, and final decisions should be submitted to the authorities. The final decision will be made whether the building can be used in its actual state, or it must be strengthened or even downgraded from a strategic building to a current building.

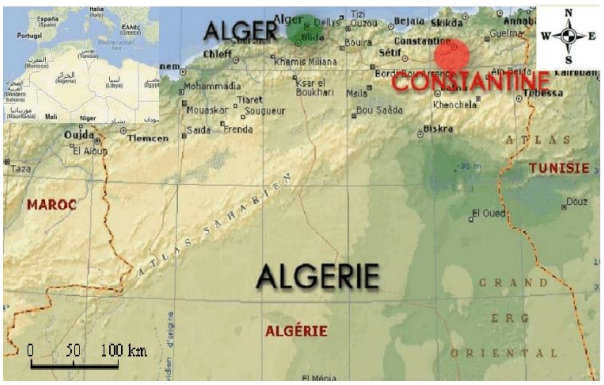

Figure 4 : Constantine location on the world map [30].

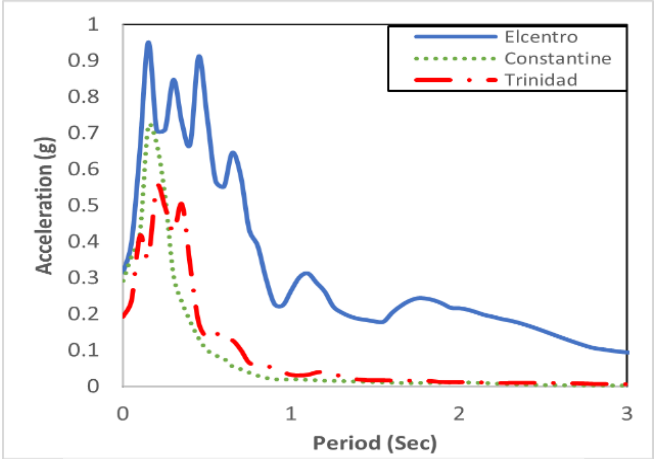

Figure 5-a : Response spectra of the selected ground motions

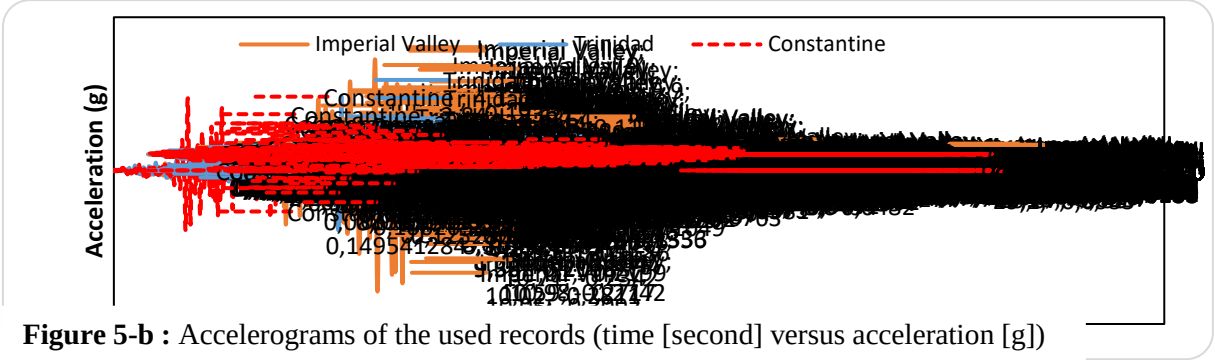

Figure 5-b : Accelerograms of the used records (time [second] versus acceleration [g])

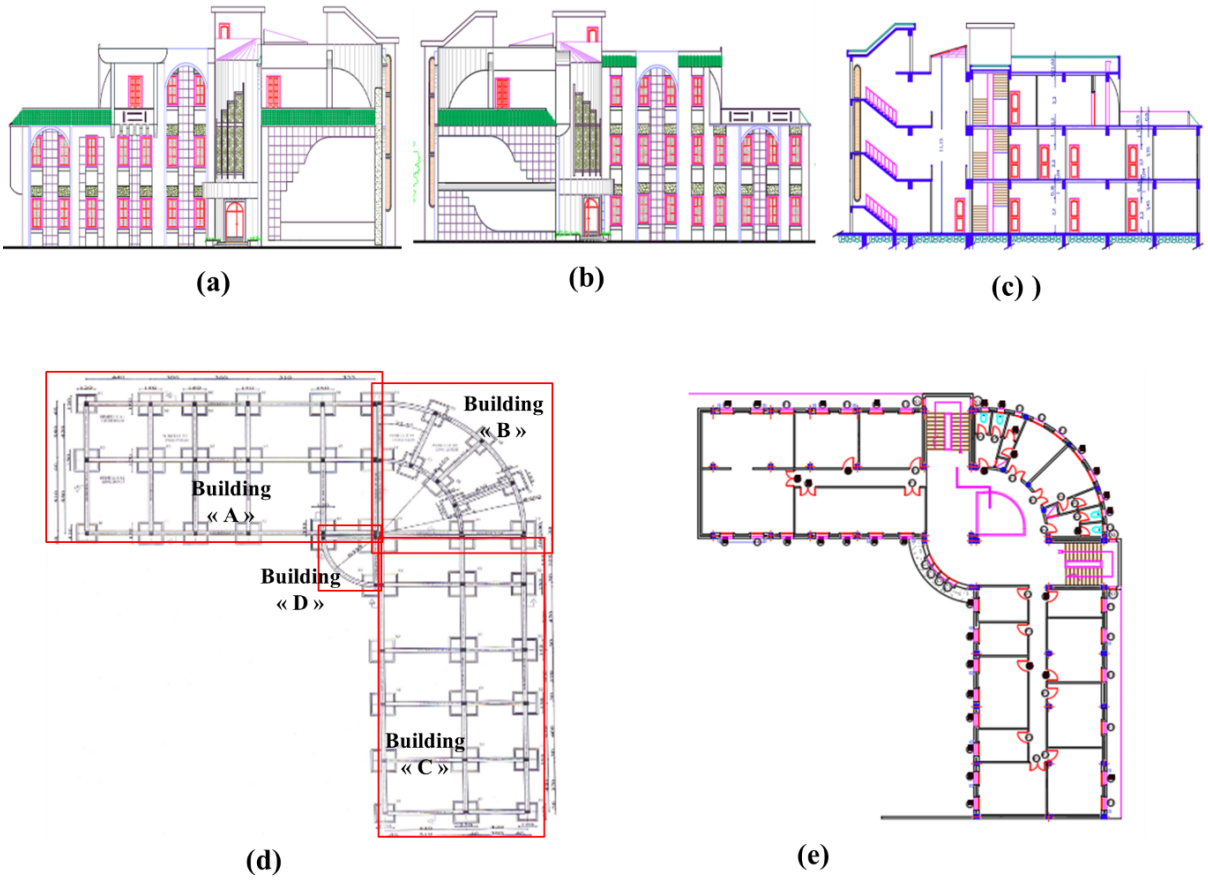

Figure 6 : Different layout of the building: a) the main façade, b) the frontal façade, c) elevation view, d) foundation plan, e) plan view (1st floor).

3- Case study: Civil protection building in Constantine (Algeria)

3.1- Description of the strategic building

The civil protection department building is composed of four (04) buildings separated by a movement joint not exceeding the 02 cm as schematized in figure 6. This structure was built in 2006. This building consists of a RC frame with masonry infill. The height of the floors is 3.06m and is identical on all three floors. The total height of the building is 9.18m from the basement level 0.00. The building is founded on six (06) simple spread footings: S1 (1.20 x1.20) m, S2 (1.50*1.50) m, S3 (1.70*1.70) m, S4 / a spread footing under two columns (2.62*2.62) m, S5 (1.50*1.20) m and S6 which is a spread footing under two columns (2.62*2.44) m. The footings are chained together by stringers of (30x40) cm² section in both directions, and there are no shear walls. The surface of the building in the plan on the 1st level is 506m², on the 2nd level 518m², the 3rd level, and the roof has a surface of 361m², and it has 31.07m of total width and 31.27m of total length.

Buildings A and C have a rectangular shape with an elevation irregularity, the two buildings have an inaccessible roof (see Fig. 6 -d).

Building A is composed of a RC concrete frame with portals in both directions. Two spans of 5.5m and 4.2m in the transverse direction. In the longitudinal direction, the portals consist of five spans of (4.55, 3, 3.6, 5.1, 3.55) m. The floors are made of hollow bodies of (16+5) thickness. They are supported by beams of (30x40) cm² in the longitudinal direction and (30x50) cm² in the transversal direction. The columns have the same dimensions (30x40) cm². The floors are tiled, the external walls and the internal partitions are made of breeze buildings.

Building B has a circular form; it is a RC frame, with two spans of 5.5m and 4.2 m in the radial direction, having square columns (30x30) and circular columns of 30 cm diameter. The floors in a hollow body of (16+5) cm thickness are

supported by beams of (30*40) in both directions. The floors with a solid slab of (12) cm thickness are supported by two types of beams, (30x40) cm. The floors are tiled, the external walls and the internal partitions are made of breeze buildings.

Building C is composed of a RC frame with portals in both directions. Two spans of 5.5m and 4.2m in the transverse direction, and in the longitudinal direction, the portals consist of five spans of (3.55, 5, 4, 4.3, 4) m.

Building D consists of a RC frame with portals in both directions.

The building D have a circular shape with a single span of 3.55m in both directions, the floors are solid slabs of (12) cm thick supported by beams (30x50). The floors are covered with tiles, the exterior wall is made of cinder building.

3.2- Mechanical Characteristics of the materials

The materials' mechanical characteristics of the four 04 buildings are mentioned in Tab.3. The steels used are mild steels FeE40 for the longitudinal and transverse reinforcements. The steel and the concrete used models are illustrated in Fig. 7 and Fig. 8 respectively.

Table 3 : mechanical characteristics of materials.

Concrete		Steel	
Comp. strength:	f_{c28} = 20 MPa	Yield strength:	f_e = 400 MPa
Tens. strength:	f_{t28} = 1.8 MPa	Yield strain:	ε_e = 2‰
Yield strain:	ε_e = 2 ‰	Ultimate strain:	ε_u = 10 ‰
Ultimate strain:	ε_u = 3.5 ‰		

3.3- Structural analysis

The fundamental periods also the nonlinear static analysis (pushover analysis) and nonlinear dynamic analysis (NLTHA) have been performed using a FEM software.

The periods of the first mode of the four buildings are represented in Tab. 4.

Table 4 : the vibration periods in both directions.

Block	Period T(sec)
A	0.526
B	0.544
C	0.532
D	0.434

3.4- Vulnerability assessment according to the Algerian seismic code "RPA99/version 2003"

The base shear force is calculated using the static equivalent force according to the Algerian seismic code, it is estimated using the following equation :

$$V = \frac{A \times D \times Q_a}{R} \times W \quad (1)$$

Where :

- V: represents the base shear force.
- A: is the acceleration coefficient of the studied zone.
- D: is the dynamic amplification factor
- Q: is the quality factor and it considers the irregularity of the building and the quality of construction and the used materials.
- R: is the behavior factor.
- W: is total weight of the building.

The shear force is distributed on the height of the building, based on the story's height and its weight the distributed horizontal forces can be calculated using the following formula:

$$Q_i = \frac{(V - F_t) \times W_i h_i}{\sum_{j=1}^{n} W_j h_j} \quad (2)$$

- Q_i: represents the horizontal force of the i^{th}story.
- V: is the total base shear force (see equation 1).
- F_t: is the horizontal concentrated force in the top floor.
- W_i: is the weight of the i^{th}story.
- n : is number of floors.

Tab.5 , Tab.6, Tab.7 and Tab.8 represent the calculated seismic lateral forces demand of each story and the stores' capacity in x-x and y-y directions. The ratio between the seismic lateral load of the i^{th} story and its capacity represents

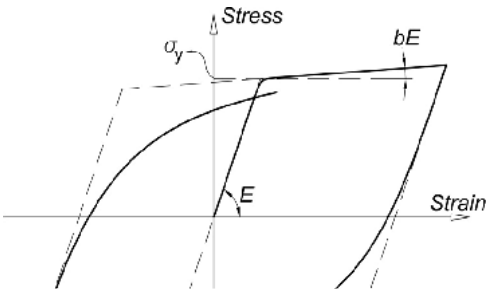

Figure 7 : Giuffré- Menegotto-Pinto Model with Isotropic Strain Hardening. [35]

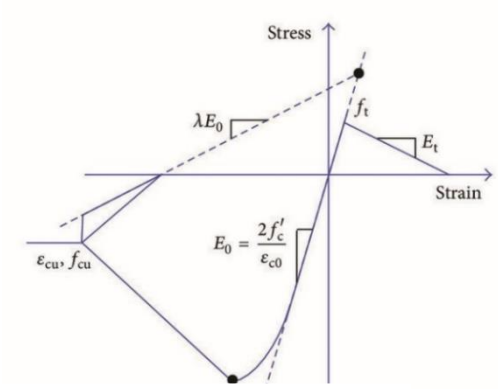

Figure 8 : Stress-strain behavior of the concrete material

Table 5 : Shear capacity; shear demand and safety factors of block A in both directions.

	X-X direction		Y-Y direction			
Story	Vi (KN)	Qi (KN)	Vi (KN)	Qi (KN)	Fs (X-X)	Fs (y-y)
3	349,44	379,96	457,33	383,68	0,91	1,19
2	825,67	839,66	899,08	832,61	0,98	1,07
1	1060,1	1086,24	1098,05	1066,19	0,97	1,02

Table 6 : Shear capacity, shear demand, and safety factors of block B in both directions.

Story	Vi (KN)	Qi (KN)	Vi (KN)	Qi (KN)	Fs (X-X)	Fs (y-y)
3	175,86	178,68	175,86	178,68	0,98	0,98
2	321,05	314,45	321,05	314,45	1,02	1,02
1	392,91	389,1	392,91	389,1	1,00	1,00

Table 7 : Shear capacity; shear demand and safety factors of block C in both directions.

Story	Vi (KN)	Qi (KN)	Vi (KN)	Qi (KN)	Fs (X-X)	Fs (y-y)
3	193,38	408,42	141,86	412,49	0,47	0,34
2	448,28	883,32	284,27	854,69	0,50	0,33
1	573,28	1137,92	349,92	1082,8	0,50	0,32

Table 8 : Shear capacity; shear demand and safety factors of block D in both directions.

	X-X direction		Y-Y direction			
Story	Vi (KN)	Qi (KN)	Vi (KN)	Qi (KN)	Fs (X-X)	Fs (y-y)
3	104,45	28,44	104,45	28,44	3,67	3,67
2	101,29	45,37	101,29	45,37	2,23	2,23
1	97,55	54,03	97,55	54,03	1,80	1,80

The safety factor F_S, this factor should always be greater than or equal 1.15 (see equation 3).

$$Fs = \frac{Qi}{Vi} \geq 1.15 \qquad (3)$$

Where :

- Q_i is the shear force capacity of the i^{th} story.
- V_i is the seismic shear force demand at i^{th} story.

3.5- Non linear dynamique response analysis

This part of the study allows the analysis of the structure to be pushed outside the linear elastic domain to simulate the real dynamic behavior of the structure, which is usually non-linear under important cyclic loads.

The analysis is performed using the CSI ETABS, which involves selected earthquake records to test the capacity of structures and their responses when excited by given ground motion records.

The displacement capacity of the different levels of each building will be compared with those requested for the selected records, which will allow knowing the dynamic behavior of the structure.

The nonlinear time history analysis (NLTHA) was performed in both X-X and Y-Y directions, using "Trinidad, Imperial- Valley, and Constantine" ground motions (see Tab.1}).

For the first level and the second level, the selected ground motions should be scaled to Amax=0.15g and Amax=0.25g respectively. The results are summarized in Tab.9, Tab.10, Tab.11, Tab.12, Tab.13 and Tab.14 . The response displacement should be compared to the maximum allowable story drift.

To achieve the above different conditions, the buildings dynamic responses must be always lower than the calculated limits (i.e.: the minimum value between the calculated capacity value and the allowable value recommended by the IIZIS/CGS methodology).

4- Fragility curves

Damage assessment aims to determine the earthquake loss for a building or group of buildings by analyzing and evaluating sufficiently detailed the vulnerability (damage) characteristics of the building/building group under a given seismic event.

To make a full vulnerability assessment, the fragility curves are needed to be constructed to give the probability of damages that can occur or happen during a specific seismic event. The Risk-UE (LM2) is a methodology that has been selected to do this analysis.

The Risk-UE level 2 method is a displacement-based method. It aims to estimate the probability of exceedance of a damage state for a given intensity measure (IM) using the fragility curves. After obtaining the pushover over curve in form of acceleration displacement response spectrum (ADRS). [32] [33]

four damage thresholds can be defined after idealizing the capacity curve (Lagomarsino and Cattari, 2013). The method uses four damage states : Minor, Moderate, Severe, and Collapse, Tab.15 illustrates the considered damage state and the mean value of each threshold.

Fragility curve can be constructed using the following equation:

$$P[d_s|S_d] = \Phi\left(\frac{1}{\beta_{ds}}.\ln\left(\frac{S_d}{\bar{S}_{d,ds}}\right)\right) \quad (4)$$

Where :

- $P[d_s|S_d]$: the probability of being in or exceeding a damage state given spectral displacement Sd.
- $\bar{S}_{d,ds}$: the mean value of each damage state (see table XV).
- β_{ds} : standard deviation of the log normal distribution.
- Φ : is the log normal distribution function.

The capacity curves and the fragility curves of the four buildings (A,B,C and D) are illustrated in Fig.9, Fig.10, Fig.11, Fig.12, Fig.13 and Fig.14. The mean values and the standard deviations of the buildings for the four damage states (slight, moderate, extensive and collapse) are represented in Tab.16.

5- Damage probabilities and damage factor

The damage probability is the difference between two fragility curves for a give intensity measurement (IM), for that reason, performance points were calculated for the building in both directions. The damage probabilities of the four buildings are calculated in Tab.17.

the repair cost can be estimated using the following equation (D'Ayala *et al*., 2015) :

$$E(C > c|IM) = \sum_{i=0}^{n} E(C > c|ds_i).P(ds_i|IM) \quad (5)$$

Where :

- n is the number of damage states considered (four damage states in our case).
- $P(ds_i|IM)$ is the probability of a building sustaining damage state ds_i.
- $\sum_{i=0}^{n} E(C > c|ds_i)$: is the complementary cumulative distribution of the cost given ds_i, the damage factors are summarized in table XVIII.
- E (C > c| IM) is the complimentary cumulative distribution of cost given a level of intensity IM (Sd).

In this case, the repair cost for this building is equal to:

- $E(C > c|S_d) = \sum_{i=0}^{n} E(C > c|ds_i).P(ds_i|Sd)$
- $= E(C > c|Slight).P(Slight|Sd) + E(C\ c|\ Moderate).P(Moderate|Sd) + E(C\ c|\ Extensive).P(Extensive|Sd) + E(C\ c|\ Complete).P(Complete|Sd)$

We consider that the buildings are subjected to IM (Sd) = [1.92, 1.96, 2.60, 2.82, 2.86, 2.40] (cm), then the resulting repair costs in term of damage factor are represented in Tab.18.

6- Discussion of the results

Based on the data presented in Tab.5, Tab.6, Tab.7, and Tab.8, it can be concluded that the shear capacity of buildings A, B, and C falls short of the demand specified by the RPA99 version 2003 at all levels. Despite this, the shear strength exceeds the demand. As a result, the safety coefficient falls below the acceptable limit of 1.15.

In the light of the results of the nonlinear dynamic response analysis which are represented in (Tab.9, Tab.10, Tab.11, Tab.11, Tab.12 and Tab.13, the displacement response of the building A, B and D are greater than the allowable inter-storey displacement. Furthermore, the joints between the different buildings are insufficient. This

Insufficiency is especially aggravated when the buildings vibrate in an opposite phase. This problem cannot be solved, even by stiffening the buildings to reduce the displacements induced by the different excitation. These displacements will always remain greater than the thickness of the joints.

According to the results obtained by calculating the repair cost in terms of damage factor, it can be concluded that buildings B and C have a repair cost that is 50% higher than that of buildings A and D. Furthermore, these two buildings do not meet the previously established acceptance criteria, including the safety factor and allowable inter-storey displacement.

Table 9 : Displacement demand and allowable inter-story displacement for building" A" (xx − direction)

story	Δ_m(mm)	Δ_M(mm)	Earthquake	Δ_m (mm)	Δ_M (mm)
3	[7,65-10,2]	[20,4-24,48]	Imperial- Val	27,1	45,2
2	[7,65-10,2]	[20,4-24,48]	Constantine	4,9	8,3
1	[7,65-10,2]	[20,4-24,48]	Trinidad	10,5	17,6

Table 10 : Displacement demand and allowable inter-story displacement for building" A" (yy − direction)

story	Δ_m(mm)	Δ_M(mm)	Earthquake	Δ_m (mm)	Δ_M (mm)
3	[7,65-10,2]	[20,4-24,48]	Imperial- Val	31,52	52,54
2	[7,65-10,2]	[20,4-24,48]	Constantine	5,76	9,601
1	[7,65-10,2]	[20,4-24,48]	Trinidad	11,50	19,17

Table 11: Displacement demand and allowable inter-story displacement for building" B" (xx and

story	Δ_m(mm)	Δ_M(mm)	Earthquake	Δ_m (mm)	Δ_M (mm)
3	[7,65-10,2]	[20,4-24,48]	Constantine	4,04	6,739
2	[7,65-10,2]	[20,4-24,48]	Imperial- Val	21,88	36,47
1	[7,65-10,2]	[20,4-24,48]	Trinidad	8,45	14,08

Table 12 : displacement demand and allowable inter-story displacement for Building C (x-x).

story	Δ_m(mm)	Δ_M(mm)	Earthquake	Δ_m (mm)	Δ_M (mm)
3	[7,65-10,2]	[20,4-24,48]	Constantine	5,131	5,131
2	[7,65-10,2]	[20,4-24,48]	Imperial- Val	3,642	3,642
1	[7,65-10,2]	[20,4-24,48]	Trinidad	1,672	1,672

Table 13 : displacement demand and allowable inter-story displacement for Building C (y-y).

story	Δ_m(mm)	Δ_M(mm)	Earthquake	Δ_m (mm)	Δ_M (mm)
3	[7,65-10,2]	[20,4-24,48]	Constantine	5,131	8,551
2	[7,65-10,2]	[20,4-24,48]	Imperial- Val	22,197	36,99
1	[7,65-10,2]	[20,4-24,48]	Trinidad	9,258	15,43

Table 14 : displacement demand and allowable inter-story displacement for Building D (x-x)/(y-y).

story	Δ_m(mm)	Δ_M(mm)	Earthquake	Δ_m (mm)	Δ_M (mm)
3	[7,65-10,2]	[20,4-24,48]	Imperial- Val	26,636	42,81
2	[7,65-10,2]	[20,4-24,48]	Constantine	4,313	7,186
1	[7,65-10,2]	[20,4-24,48]	Trinidad	10,177	16,96

Table 15 : Median value of spectral displacement.

Damage state label	Damage state Thresholds	Spectral displacement
Slight	$\bar{S}_{d1}$	$0.7\ D_y$
Moderate	$\bar{S}_{d2}$	D_y
Extensive	$\bar{S}_{d3}$	$D_y + 0.25(D_u - D_y)$
collapse	$\bar{S}_{d4}$	D_u

Table 16 : Mean and standard deviation values in (cm)

Block	Direction	Slight		moderate		extensive		collapse	
		$\bar{S}_{d,1}$	β_{ds}	$\bar{S}_{d,2}$	β_{ds}	$\bar{S}_{d,3}$	β_{ds}	$\bar{S}_{d,4}$	β_{ds}
A	XX	1,127	0,384	1,61	0,409	4,64	0,700	13,76	0,862
	YY	0,728	0,283	1,04	0,302	2,92	0,912	8,57	0,854
B	XX / YY	0,567	0,283	0,81	0,302	2,29	0,914	6,73	0,856
C	XX	0,777	0,283	1,11	0,302	3,37	0,939	10,24	0,877
	YY	0,574	0,283	0,82	0,302	2,69	0,955	8,31	0,895
D	XX / YY	1,316	0,310	1,88	0,192	2,325	0,193	3,66	0,360

Table 17 : Damage probability matrix

Block	Direction	Performance point (Sd) in cm	Slight (%)	moderate (%)	extensive (%)	collapse (%)
A	XX	1,92	34,47	35,52	4,42	0,46
	YY	1,96	12,50	64,52	20,36	1,91
B	XX / YY	2.60	2,56	66,36	27,35	3,70
C	XX	1.82	17,06	63,09	17,21	1,31
	YY	18.6	2,80	71,12	23,43	2,59
D	XX / YY	2.40	53,67	8,46	0,23	0,53

Table 18 : Damage factor values [34]

Reference	Damage state			
	Slight	Moderate	Extensive	Collapse
Bal et al (2008)	16%	33%	105%	104%

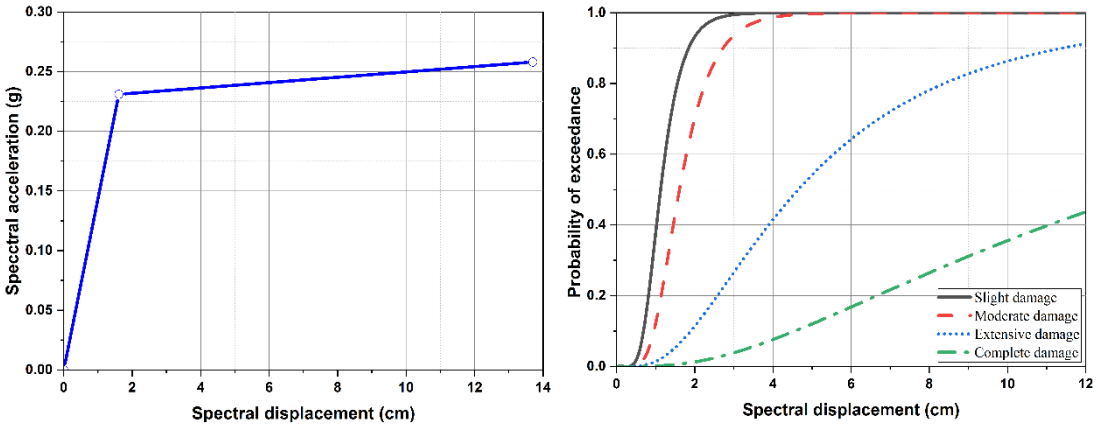

Figure 9 : Capacity curve and fragility curves of the building “A" (x-x direction)

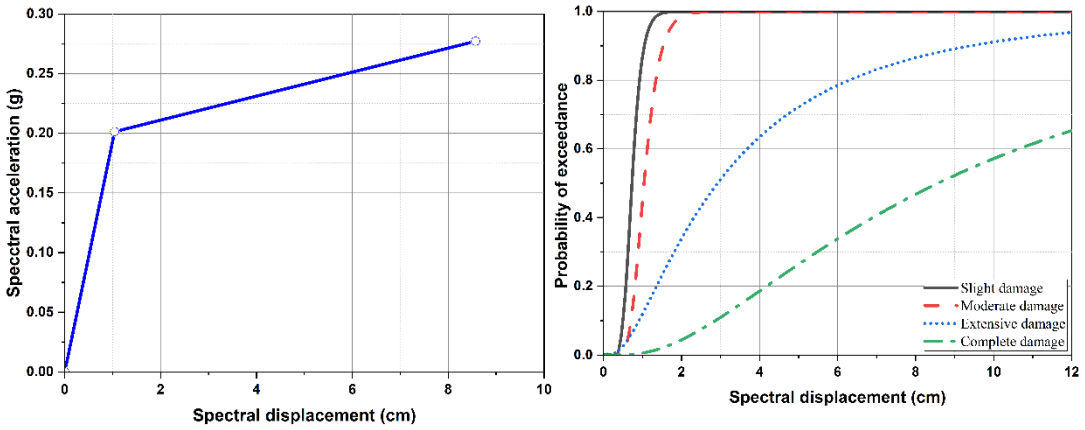

Figure 10 : Capacity curve and fragility curves of the building “A" (y-y direction)

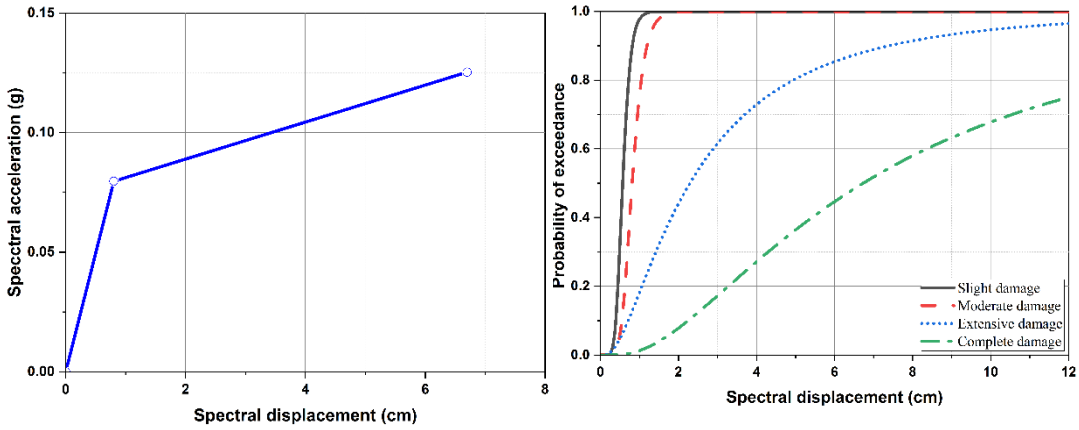

Figure 11 : Capacity curve and fragility curves of the building “B" (x-x and y-y direction)

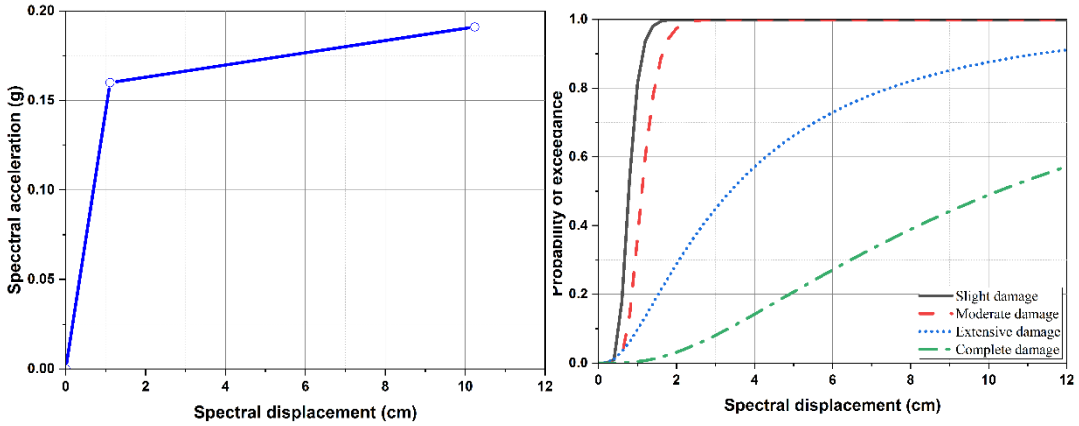

Figure 12: Capacity curve and fragility curves of the building “C" (x-x direction).

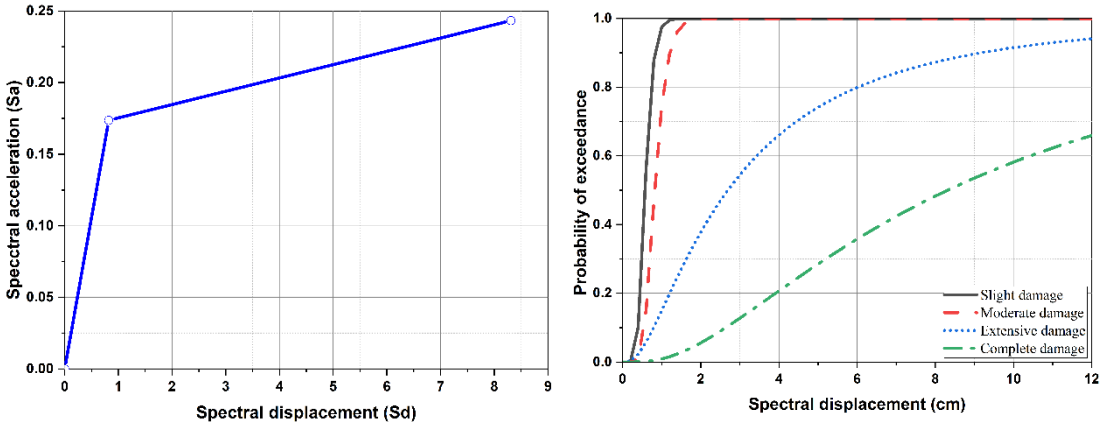

Figure 13: Capacity curve and fragility curves of the building “C" (y-y direction).

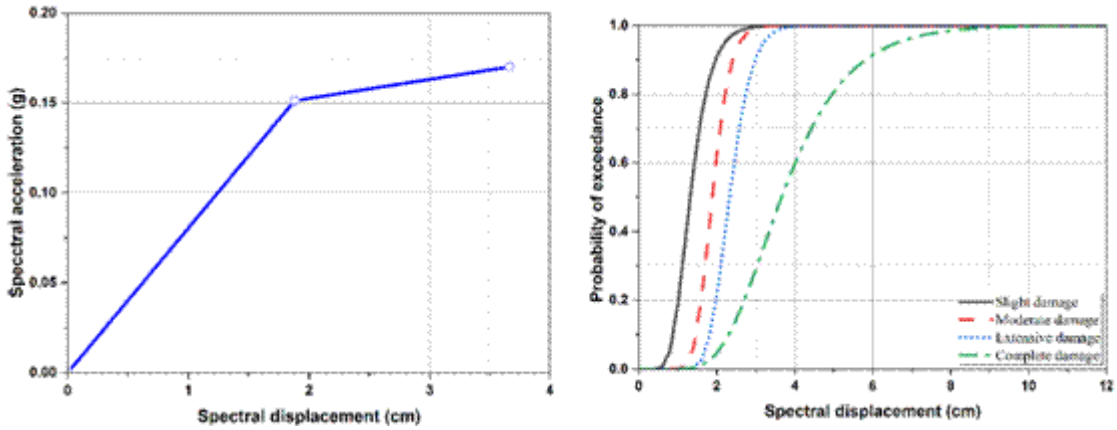

Figure 14: Capacity curve and fragility curves of the building “D" (x-x and y-y direction)

7- Conclusion

In this study, the seismic vulnerability and fragility of an existing strategic reinforced concrete frame structure (civil protection department) were evaluated using the IZIIS/CGS methodology. The aim was to assess the structure's functionality and behaviour during and after an earthquake event.

The analysis began with a static analysis to determine the capacity of buildings A, B, C, and D in both the x-x and y-y directions. The resulting safety factor was compared to the factor recommended by the Algerian seismic regulation (RPA 99 version 2003), and it was found that buildings A, B, and C did not meet this requirement.

Next, a nonlinear dynamic analysis was conducted on these buildings in both directions to evaluate the displacement of each floor against the allowable inter-story displacement recommended by the methodology. It was found that the inter-story displacement of buildings A, B, and D was below the acceptable criterion.

Finally, fragility curves were constructed, and damage probabilities were calculated. To better understand the estimated post-seismic damage, a damage factor was included in the methodology to provide authorities with an understanding of the financial implications of strengthening the structure. This factor represents the ratio of repair costs to the cost of a new building. Buildings A, B, and C had the highest repair costs relative to the cost of a new building, at 46%, 54%, and 51%, respectively.

In conclusion, the Department of Civil Protection building does not meet the requirements for resistance and deformability recommended by the CGS/IIZIS methodology for the group of users it serves. Therefore, it is suggested that the building's function be changed from a strategic building to a standard structure in order to downgrade its classification.

Références bibliographiques

[1] C. Zhai, . Y. Zhao, W. Wen, . H. Qin and L. Xie, “A novel urban seismic resilience assessment method considering the weighting of post-earthquake loss and recovery time,” *International Journal of Disaster Risk Reduction*, vol. 84, p. 103453, 2023.

[2] M. Mavrouli, S. Mavroulis, E. Lekkas and A. Tsakris, “The impact of earthquakes on public health: A narrative review of infectious diseases in the post-disaster period aiming to disaster risk reduction,” *Microorganisms*, vol. 11, p. 419, 2023.

[3] Y. Rong, D. D. Jackson and Y. Y. Kagan, “Seismic gaps and earthquakes,” *Journal of Geophysical Research: Solid Earth*, vol. 108, 2003.

[4] A. Ayadi, F. Ousadou-Ayadi, S. Bourouis and H. Benhallou, “Seismotectonics and seismic quietness of the Oranie region (Western Algeria): The Mascara earthquake of August 18 th 1994, M w= 5.7, M s= 6.0,” *Journal of Seismology*, vol. 6, p. 13–23, 2002.

[5] R. Ouyed, M. S. Boughacha, M. Bezzeghoud and Vavry, “Fault plane picking from focal mechanisms in reverse faulting stress: Application to the Mw6. 9 Boumerdes (Algeria) earthquake sequence,” *Journal of African Earth Sciences*, vol. 196, p. 104729, 2022.

[6] X. Liu, Z. Jiang and . H. A. Mang, “Experimental investigation of the bearing capacity of deformed segmental tunnel linings strengthened by a special composite structure,” *Structure and Infrastructure Engineering*, vol. 3, pp. 147--163, 2023.

[7] H. Ritchie and M. Roser, “Natural disasters,” *Our World in Data*, 2014.

[8] M. Mouhine and E. Hilali, “Seismic vulnerability assessment of RC buildings with setback irregularity,” *Ain Shams Engineering Journal*, vol. 13, p. 101486, 2022.

[9] M. Stepinac and M. Gašparović, "A review of emerging technologies for an assessment of safety and seismic vulnerability and damage detection of existing masonry structures," *Applied Sciences*, vol. 10, p. 5060, 2020.

[10] J. Huh, Q. H. Tran, A. Haldar, I. Park and J.-H. Ahn, "Seismic vulnerability assessment of a shallow two-story underground RC box structure," *Applied Sciences*, vol. 7, p. 735, 2017.

[11] M. M. Kassem, F. M. Nazri and E. N. Farsangi, "The seismic vulnerability assessment methodologies: A state-of-the-art review," *Ain Shams Engineering Journal*, vol. 11, p. 849–864, 2020.

[12] M. Boukri, M. N. Farsi, A. Mebarki, M. Belazougui, M. Ait-Belkacem, N. Yousfi, N. Guessoum, D. A. Benamar, M. Naili, N. Mezouar and others, "Seismic vulnerability assessment at urban scale: Case of Algerian buildings," *International journal of disaster risk reduction*, vol. 31, p. 555–575, 2018.

[13] B. SAHIN, M. BRAVO-HARO and A. Y. ELGHAZOULI, "Cyclic modelling of composite steel-concrete members," in *Earthquake Risk and Engineering Towards a Resilient World SECED2019*, Greenwich London, 2019.

[14] R. Leslie and A. Naveen, "A study on pushover analysis using capacity spectrum method based on Eurocode 8," in *16th World Conference on Earthquake Engineering, Reg Code: S-P148645023, Santiago, Chile*, 2017.

[15] N. ekta and O. Kegyes-Brassai, "Development in Fuzzy Logic-Based Rapid Visual Screening Method for Seismic Vulnerability Assessment of Buildings," *Geosciences*, vol. 3, p. 13, 2023.

[16] Y. Aggarwal and S. K. Saha, "An improved rapid visual screening method for seismic vulnerability assessment of reinforced concrete buildings in Indian Himalayan region," *Bulletin of Earthquake Engineering*, vol. 21, pp. 319--347, 2023.

[17] S.-Q. Li, Y.-S. Chen, H.-B. Liu and C. Del Gaudio, "Empirical seismic vulnerability assessment model of typical urban buildings," *Bulletin of Earthquake Engineering*, pp. 1-4, 2023.

[18] M. Yekrangnia, "Seismic Vulnerability Assessment of Masonry Residential Buildings in the Older Parts of Tehran through Fragility Curves and Basic RVS Scores," *Buildings*, vol. 13, p. 302, 2023.

[19] B. Liang, J. Hou and . Z. He, "Rapid assessment method to assess vulnerability of structures using vulnerability index and disaster matrix," *Bulletin of Earthquake Engineering*, pp. 1--32, 2023.

[20] M. Biglari, A. Formisano and A. Davino, "eismic vulnerability assessment and fragility analysis of Iranian historical mosques in Kermanshah city," *Journal of Building Engineering*, vol. 45, p. 103673, 2022.

[21] F. Lazzali, "Seismic vulnerability analysis of RC buildings: Case study of Ibn Khaldoun area in Boumerdes city, Algeria," *Jordan Journal of Civil Engineering*, vol. 15, 2021.

[22] S. Fallah-Aliabadi, . A. Ostadtaghizadeh, . A. Ardalan, M. Eskandari, . F. Fatemi, . M. R. Mirjalili and . B. Khazai, "Risk analysis of hospitals using GIS and HAZUS: A case study of Yazd County, Iran," *International Journal of Disaster Risk Reduction*, vol. 47, p. 101552, 2019.

[23] Gandage and . M. Goel, "Seismic Fragility Assessment of RC Building Using HAZUS Methodology and Incremental Dynamic Analysis," *ASPS Conference Proceedings*, vol. 1, pp. 731--738, 2022.

[24] D. Zebua, "Performance Evaluation of Highrise Building Structure Based on Pushover Analysis with ATC-40 Method," *Applied Research on Civil Engineering and Environment (ARCEE),* vol. 3, pp. 54--63, 2022.

[25] F. Kehila, M. Remki and K. Abderrahmane , "Developing seismic fragility curves for existing reinforced concrete structures in Algeria," *Proceedings of the Institution of Civil Engineers-Structures and Buildings,* vol. 175, pp. 418--433, 2022.

[26] M. Kutanis, H. Ulutaş and E. Işik, "PSHA of Van province for performance assessment using spectrally matched strong ground motion records," *Journal of Earth System Science,* vol. 127, p. 1–14, 2018.

[27] M. Keller, A. Pasanisi, M. Marcilhac, T. Yalamas, R. Secanell and G. Senfaute, "A Bayesian methodology applied to the estimation of earthquake recurrence parameters for seismic hazard assessment," *Quality and Reliability Engineering International,* vol. 30, p. 921–933, 2014.

[28] S. Maouche, Y. Bouhadad, A. Harbi, Y. Rouchiche, F. Ousadou and A. Ayadi, "Active tectonics and seismic hazard in the Tell Atlas (Northern Algeria): a review," *The Geology of the Arab World—An Overview,* p. 381–400, 2019.

[29] A. Yelles-Chaouche, T. Allili, A. Alili, W. Messemen, H. Beldjoudi, F. Semmane, A. Kherroubi, H. Djellit, Y. Larbes, S. Haned and others, "The new Algerian Digital Seismic Network (ADSN): towards an earthquake early-warning system," *Advances in Geosciences,* vol. 36, p. 31–38, 2013.

[30] M. Boukri, M. N. Farsi, A. Mebarki, M. Belazougui, O. Amellal, B. Mezazigh, N. Guessoum, H. Bourenane and A. Benhamouche, "Seismic risk and damage prediction: case of the buildings in Constantine city (Algeria)," *Bulletin of earthquake engineering,* vol. 12, p. 2683–2704, 2014.

[31] P. Center, "PEER Ground Motion Database - PEER Center," 5 5 2023. [Online]. Available: https://ngawest2.berkeley.edu/.

[32] D. Kazantzidou-Firtinidou, P. Lestuzzi, S. Podestà, C. Luchini and C. Bozzano, "Improvement of Risk-UE LM2 capacity curves for reliable seismic vulnerability assessment at urban scale in Switzerland," in *Proceedings of the 1st International Conference on Natural Hazards & Infrastructures, ICONHIC 2016*, 2016.

[33] N. Bektaş and O. Kegyes-Brassai, "Conventional RVS Methods for Seismic Risk Assessment for Estimating the Current Situation of Existing Buildings: A State-of-the-Art Review," *Sustainability,* vol. 14, p. 2583, 2022.

[34] A. H. Barbat, L. G. Pujades and N. Lantada, "Seismic damage evaluation in urban areas using the capacity spectrum method: application to Barcelona," *Soil Dynamics and Earthquake Engineering,* vol. 28, p. 851–865, 2008.

[35] H. Ebrahimian, R. Astroza, J. P. Conte and R. A. de Callafon, "Nonlinear finite element model updating for damage identification of civil structures using batch Bayesian estimation," *Mechanical Systems and Signal Processing,* vol. 84, p. 194–222, 2017.